Visible and near infrared emissions of Barium-Yttrium-Fluoride crystals doped with holmium ions

Taiju TSUBOI[1)]
Silviu POLOSAN[1)]
Kiyoshi SHIMAMURA[2)]
Hyo-Jin SEO[3)]
Marco BETTINELLI[4)]

[1)] Faculty of Computer Science and Engineering, Kyoto Sangyo University, Kyoto 603-8555, Japan
[2)] Optronic Materials Center, National Institute for Materials Science, Tsukuba 305-0044, Japan
[3)] Department of Physics, Pukyong National University, Busan 608-737, Republic of Korea
[4)] Laboratory of Solid State Chemistry, Department of Biotechnology, University of Verona and INSTM, UdR Verona, 37134 Verona, Italy

Abstract

The ultraviolet, visible, and near infrared (800-2400 nm) luminescence spectra of barium-yttrium-fluoride (BaY_2F_8) single crystals heavily doped with the holmium ions (10 and 30 mol %) have been investigated at room temperature and 12 K, together with the luminescence decay curves (up to 300 μs) of the visible emission. Excitation in the visible region gives rise to very strong emission bands originating from the first $^5I_7$ level and located around 2070 nm. However the $^5I_7$ emission is not observed upon excitation at wavelengths shorter than 300 nm presumably because at the present doping levels cross relaxation processes bypass the $^5I_7$ level without populating it. The inter-ionic processes are found to shorten the decay times of the levels emitting in the visible region with respect to the corresponding radiative lifetimes.

1. Introduction

Rare-earth-doped materials have been used for various applications in opto-electronics. For example, erbium-doped materials are used for optical amplifier for optical fiber communications and for solid state laser. The reason is that Er^{3+} ion gives intense and broad emission band at about 1.5 μm due to the $^4I_{13/2} \rightarrow {}^4I_{15/2}$ transition in addition to green emission as seen in Fig.1 where

photoluminescence (PL) spectra of Er^{3+} ions doped in yttrium lithium fluoride ($LiYF_4$, called YLF) crystal are presented.

On the other hand, holmium ion (Ho^{3+}) doped crystals play an important role in practical applications including medicine and eye-safe remote sensing system, coherent Doppler velocimetry and gas detection [1], because Ho^{3+} ions doped in insulating crystals give strong emission in the near infrared range of 1900-2100 nm [2, 3, 4]. This emission is caused by the electronic transition $^5I_7 \rightarrow {}^5I_8$ in Ho^{3+} ions. The Ho^{3+} infrared emission has been confirmed to give laser action in various host crystals since early work on $LiYF_4$:Ho^{3+} [5, 6]. The spectral region around 2 μm is absorbed by liquid water. Therefore, Ho-laser is used as eye-safe laser in medical treatment for patients with superficial bladder carcinoma [2] and for eye posterior segment surgery [7]. The Ho-laser is also useful for laser radar imaging because the light around 2 μm shows high atmospheric transmittance and low background noise [8].

A high performance of the near-infrared Ho^{3+} laser action is requested for the practical applications and in turn this implies an intense luminescence from the Ho^{3+} dopant ions. Among the concepts that have been suggested to enhance the luminescence intensity, change of host crystal, change of pumping source including the excitation wavelength, and increase in concentration of Ho^{3+} ions doped in host crystal are probably prominent. Most luminescence studies have been carried out for crystals with relatively low Ho^{3+} concentrations around 0.5 - 5 mol %, in order to avoid concentration quenching. Few studies have been made in a wide spectral region spanning ultraviolet, visible and near infrared.

The present study was undertaken to investigate the characteristics of infrared emission bands of heavily Ho^{3+} -doped crystals, together with visible Ho^{3+} emission bands. We have chosen to investigate the luminescence spectra of monoclinic crystals of barium-yttrium-fluoride (BaY_2F_8) singly doped with 10 and 30 % Ho^{3+} ions in a wide spectral region of ultraviolet, visible and near infrared. The optical spectroscopy of BaY_2F_8 fluoride crystal doped with Ho^{3+} ions has already been studied [9], and this material has been shown to be an efficient laser crystal [10]. In this paper we extend the previous investigations to crystals more heavily doped (i.e., 10 and 30 mol %).

2. Experimental procedure

Single crystals of heavily Ho^{3+} -doped BaY_2F_8 were grown by the Czochralski method [11]. The crystal growth was carried out with a 30 kW radio frequency generator. High purity powders (>99.99%) of commercially available BaF_2, YF_3, and HoF_3 were utilized. BaF_2 and YF_3 were weighed and mixed in stoichiometric amounts. The concentrations of Ho^{3+} ions in BaY_2F_8 were 10 and 30

mol % in the melt. Purification of the raw materials was carried out in a platinum/graphite crucible, heating at 700 ℃ for a period of 12 hours under vacuum of approximately 10^{-3} Pa. This vacuum level, obtained by a rotary and a diffusion pump, was necessary to eliminate effectively the water and oxygen present in the chamber and raw materials, since even traces of those compounds are well known to be very detrimental for the optical quality of fluoride crystals. Subsequently, high purity CF_4 gas (99.99 %) was slowly flowed into the furnace and the powders were melted at about 985 ℃. After seeding, crystal rotation and pulling rates were fixed at 10 rpm and 1 mm/h, respectively.

A heavily doped Ho^{3+} (35 mol %)-doped CaF_2 crystal was also grown for comparison using methods previously described [12].

Absorption spectra were measured with a Shimadzu UV-3100 spectrophotometer at room temperature. Luminescence spectra were measured with a Horiba Spex Fluorolog-3 spectrophotometer at room temperature and 12 K. Infrared spectra were measured in a spectral range between 800 to 2500 nm using a liquid-nitrogen cooled Jobin-Yvon DSSX-IGA010L InGaAs photo-diode. Light from a 450 W Xenon lamp was used to excite the crystals.

High resolution spectra (Fig. 9) and decay curves (Figs. 10 and 11) were obtained as follows. The excitation source is a Dye laser (Spectron Laser Sys. SL4000) pumped by the third harmonic (355 nm) of a pulsed Nd:YAG laser (Spectron Laser Sys. SL802G). The laser beam was focused inside the sample with a cross-sectional area of about 3 mm^2. The pulse energy was about 5 mJ with 10 Hz repetition rate and 5 ns duration. The luminescence was dispersed by a 75 cm monochromator (Acton Research Corp. Pro-750) and observed with a photomultiplier tube (PMT) (Hamamatsu-Photonics R928). The luminescence decay was averaged for 1000 laser pulses (10 Hz repetition rate) and the number of data points was about 10^4. The slit widths of the monochromator were normally set to give a resolution of 0.2 nm during decay measurements. The time-integrated emission spectrum was detected with a spectral resolution of 0.10 nm and a scanning step of 0.025 nm. The data points in the time-integrated emission spectrum were obtained by integration of the averaged decays for 10 laser pulses observed in the oscilloscope at the individual steps of the wavelength scan.

3. Experimental results and discussion

BaY_2F_8 has a monoclinic crystal structure, with space group C_{2h}^3-C_2/m and lattice parameters a=6.9829Å, b=10.5190Å, c=4.2644Å, $\alpha=\gamma=90°$, $\beta=99.676°$ [13]. The barium and yttrium cations are located in one site each, corresponding to BaF_{12} and YF_8 polyhedra with point group symmetries C_{2h} and C_2, respectively. Vibrational spectra have shown that the maximum phonon energies of the

BaY_2F_8 host are located at about 420-440 cm^{-1} [13, 14]. The phonon energies values are relatively low; this makes multiphonon relaxation inefficient in this host crystal.

The ionic radius of Ho^{3+} is very similar to the one of Y^{3+} (1.015 and 1.019 Å, respectively, for 8-fold coordination [15]), whilst Ba^{2+} is significantly larger (ionic radii 1.42 and 1.61 Å for 8-fold [15] and 12-fold coordination [16], respectively). It is reasonable to assume that in the crystals under investigation the Ho^{3+} ions will be mainly located in the Y^{3+} sites (C_2 symmetry), even though at the present concentrations some minority accommodation of Ho^{3+} in the Ba^{2+} site (C_{2h} symmetry) cannot be ruled out.

Figure 2 shows the absorption spectra of the 30 % Ho^{3+} -doped BaY_2F_8 crystal in the ultraviolet-visible and near infrared ranges at room temperature. The crystals doped with 10 and 30 % Ho^{3+} ions do not show any host absorption in 190 - 3100 nm spectral range. Sharp absorption bands due to Ho^{3+} appear in the ultraviolet-visible-infrared range between 200 and 2200 nm. All the bands agree with the Dieke energy level diagram of trivalent Ho^{3+} ($4f^{10}$) ion [17]. For example, absorption bands due to the $^5I_8 \rightarrow {}^3K_7 + {}^5G_4$ transitions are observed at 386 and 392 nm, respectively. Among the Ho^{3+} absorption bands located in the UV and visible spectral ranges, the weakest feature is observed at 745 - 770 nm due to the $^5I_8 \rightarrow {}^5I_4$ transition (Fig. 2(a)). Three infrared absorption bands appear at 880 - 920, 1135 - 1205, and 1850 - 2095 nm, which are due to the $^5I_8 \rightarrow {}^5I_5$, $^5I_8 \rightarrow {}^5I_6$, and $^5I_8 \rightarrow {}^5I_7$ transitions, respectively (Fig. 2(b)). The assigned energy levels and the absorption transitions are shown in Fig. 3(a).

The four Ho^{3+} absorption bands corresponding to the $^5I_8 \rightarrow {}^5I_4$, $^5I_5$, $^5I_6$, and $^5I_7$ transitions exhibit increase of band intensity on going from short wavelength to long wavelength, i.e., the 745-770 nm ($^5I_4$) band is the weakest, while the 1850 - 2095 nm ($^5I_7$) band is the strongest (Figs. 2(a) and 2(b)). This behaviour can be explained by considering that the electric dipole oscillator strength of the $^5I_8 \rightarrow {}^5I_n$ (n=4, 5, 6 and 7) is given by the Judd-Ofelt theory, and is proportional to the square of the matrix elements of the unit tensor operators $U^{(\lambda)}$. These values, for λ =2, 4 and 6 for the transitions of interest here, effectively increase with n increasing from 4 to 7 [18]. Moreover, the $^5I_8 \rightarrow {}^5I_7$ transition has also a contribution due to the magnetic dipole mechanism, as it is characterized by $|\Delta J|=1$.

Figure 4 shows the luminescence spectrum of 10% Ho^{3+} -doped BaY_2F_8 crystal excited at 285 nm at room temperature. The emission bands can be assigned on the basis of the energy level diagram obtained from the absorption spectra. It is noted that the band at about 2070 nm, corresponding to the $^5I_7 \rightarrow {}^5I_8$ transition (see Fig. 3(b)), is the dominant feature located in the near infrared region (Fig. 4 (b)). The relative intensity of the $^5I_6 \rightarrow {}^5I_8$ emission transition, with respect to the $^5I_7 \rightarrow {}^5I_8$ one, is much smaller than for the corresponding band in the absorption spectrum.

Figure 5 presents the luminescence spectra, in a visible spectral range, of 30% Ho^{3+} -doped BaY_2F_8 crystal excited at 450 nm at various temperatures between 287 K and 12 K. All the emission bands show increase of the intensity, narrowing, and splitting into several lines with decreasing temperature from 287 K, except the emission band near 635 nm. For example, the 491 nm and 550 nm peaks increase the height by about 5.3 times at 12 K, while the 660 nm peak by 11.2 times. Additionally new emission lines appear at 484, 486, 541, 543, and 647 nm.

Figure 6 shows the luminescence spectra, in a near infrared spectral range, of 30% Ho^{3+} -doped BaY_2F_8 crystal excited at 360 nm at various temperatures between 270 K and 12 K. Like the case of visible emission bands, all the emission bands show increase of the intensity with decreasing temperature.

The excitation spectra for 660 nm and 2070 nm emissions are shown in Fig. 7 for the crystal containing 10% Ho^{3+}. The excitation spectra exhibit similar spectral features to the absorption spectrum (Fig. 2 (a)), but the relative intensities and spectral features in each band do not exactly match those of the bands in the absorption spectrum because the excitation spectra reflect the probabilities of population of the $^5F_5$ (emission at 660 nm) and $^5I_7$ (emission at 2070 nm) levels. It is interesting to note that the absorption bands in the spectral region 210 - 300 nm, corresponding to transitions from the $^5I_8$ ground state to excited levels from $^5D_3$ upwards [19, 20], disappear in the excitation spectrum for the 2070 nm emission (Fig. 7 (a)), whilst they are observed in the excitation spectrum for the 660 nm emission (Fig. 7 (b)).

This result indicates that the high energy excitation presumably gives rise to relaxation to the lower energy states accompanied by emission of phonons in part and then nonradiative relaxation again to the next lower energy levels or radiative transition to the ground state ($^5I_8$) with photon emission. Cross-relaxation and migration between Ho^{3+} ions can also be involved in the relaxation processes. In the case of excitation at wavelengths lower than 300 nm, all the excitation energy is relaxed bypassing the $^5I_7$ level resulting in no excitation band in that spectral range for 2070 nm emission differently from the excitation spectrum for 660 nm emission.

Figures 8 (a) and 8 (b) show excitation spectra of 30% Ho^{3+} -doped BaY_2F_8 for 2070 nm emission at 12 K and room temperature, respectively. The 2070 nm $^5I_7$ emission is not observed upon excitation at wavelengths shorter than 300 nm, as observed in the case of the 10 % Ho^{3+} crystal. Each excitation band at room temperature has shoulder at the longer wavelength side as indicated by dotted lines in Fig. 8 in comparison with the band obtained at 12 K. The average energy difference between the shoulders of each band obtained at 12 K and room temperature is estimated to be about 410 cm^{-1}. The ground $^5I_8$ multiplets split into seventeen (2J+1) Stark levels for C_2 crystal field symmetry of Ho^{3+} (supposed to replace Y^{3+}). The energy difference between the

lowest and the highest Stark levels of Ho^{3+} ($^5I_8$) is reported to be 371 cm^{-1} in BaY_2F_8 [21], which is close to the average energy difference of shoulders (410 cm^{-1}). The crystal field splitting of the $^5I_8$ multiplet depends on the host lattices, e.g., 530 cm^{-1} in $Y_3Al_5O_{12}$, 315 cm^{-1} in $LiYF_4$, and 420 cm^{-1} in CaF_2. At room temperature, the excitation can occur from thermally populated higher Stark levels from the lowest Stark level of the $^5I_8$ ground state. This is the reason why we observe the shoulders appearing at lower energy side of each excitation feature.

From the energy level diagram, it is possible to attribute the 2070 nm emission to the $^5F_3 \rightarrow {}^5F_5$ or $^5F_4 \rightarrow {}^5I_5$ transition. Excitation at about 650 nm, however, gives rise to the 2 μm emission (Figs. 7 and 8). Therefore it is concluded that the radiative transition from not the $^5F_3$ and $^5F_5$ excited states but the $^5I_7$ is responsible for the infrared emission (Fig. 3 (b)).

Figure 9 shows the luminescence spectra of heavily Ho^{3+} -doped BaY_2F_8 crystals in near the infrared region at 12 K with excitation at 447 nm. A very strong emission is observed at around 2 μm, whilst the emission bands at around 980 nm and 1470 nm are much weaker than another less intense emission band at 1200 nm. Upon 447 nm excitation at 12 K the ratios of the 1.2 μm emission intensity ($^5I_6 \rightarrow {}^5I_8$ transition) to the 2 μm emission intensity ($^5I_7 \rightarrow {}^5I_8$ transition) are estimated to be 0.22 and 0.045 for 10% Ho^{3+} -doped BaY_2F_8 and 30% Ho^{3+} -doped BaY_2F_8, respectively. When excited at 533 nm, almost the same infrared luminescence spectra were observed (not shown in the figure). These results clearly indicate that energy transfer processes depopulate the $^5I_6$ level in the heavily doped crystals.

In addition to the emission bands in the 1135-1205 and 1850-2095 nm regions, very weak and sharp emission bands around 980 and 1470 nm are observed in 30% Ho^{3+} -doped BaY_2F_8 crystals, but not in 10% Ho^{3+} -doped BaY_2F_8 crystal, as shown in Fig.7. These 980 and 1470 nm emission bands for the 30% Ho^{3+} -doped BaY_2F_8 crystal are observed upon excitation at 359, 450, 480 and 645 nm, but not upon excitation at 535 nm (corresponding to excitation into the $^5S_2$ state of single Ho^{3+} ions). On the basis of the energy level scheme of the Ho^{3+} ion, it is possible to assign the 980 and 1470 nm bands to the $^5F_5 \rightarrow {}^5I_7$ and $^5F_5 \rightarrow {}^5I_6$ transitions, respectively. Therefore, taking into account that these emissions are only observed in 30% Ho^{3+} -doped crystals, it is suggested that they are attributed to a concentration dependent phenomenon, such as the occupation of the Ba^{2+} site and/or the formation of Ho^{3+} -pairs or clusters. This is consistent with the observation of emission bands due to Ho^{3+} -pairs in the same spectral regions in heavily 35% Ho^{3+} -doped CaF_2 (see Fig. 9 (b)) [22].

The highly resolved luminescence spectrum of the 10 % Ho^{3+} -doped BaY_2F_8 crystal measured at 17 K upon excitation at 355 nm is shown in Fig. 10. Decay curves corresponding to several emission wavelengths are shown in Fig. 11. Longer decay curves were observed for the 375.2, 377.6, 541.8, 551.6, 647.4, and 660.2 nm emission lines, while shorter curves for the 391.0, 422.2,

485.4, 491.6, 580.6, and 586.0 nm lines. Therefore the measurement was done in time scales of 0-300 and 0-18 μs for the former and latter lines, respectively.

The strong emission lines located around 550 nm are assigned to the $^5S_2 \rightarrow {}^5I_8$ transition. The corresponding decay curves of the thermalized ($^5F_4$, $^5S_2$) levels measured at 17 K at 541.8 and 551.8 nm are characterized by a measurable rise with a time constant of about 7 μs and a non-exponential decay with a 1/e decay time of about 35 μs. The luminescence rise can be explained by a slow feeding of the emitting state from the higher lying state ($^5F_4$, $^5S_2$) populated by the 355 nm exciting radiation. The non-exponential shape of the decay part of the curve is attributed to Ho^{3+} -Ho^{3+} energy transfer processes; the value of the decay time constant can be compared to the radiative decay time of the thermalized ($^5F_4$, $^5S_2$) levels calculated on the basis of the Judd-Ofelt theory (317 μs) [9] indicating that concentration quenching strongly affects this excited state.

We note that the emission lines at 375.2 and 377.6 nm are characterized by decay curves very similar to the ones observed for the ($^5F_4$, $^5S_2$) excited state. These emission features could be assigned as originating from the $^5G_4$ level, but the observation that the decay time is in practice identical to the one of ($^5F_4$, $^5S_2$) may also suggest an alternative explanation. In fact BaY_2F_8:Ho^{3+} crystals are characterized by efficient upconversion processes [21, 23] and UV upconversion of Ho^{3+} has been very well documented [24-26]. It is therefore conceivable that the intense laser excitation gives rise to upconverted emission from highly excited states, with the thermalized metastable ($^5F_4$, $^5S_2$) levels as intermediate states. In this case the upconverted emission would have the same decay as the feeding metastable level.

The strong emission appearing around 650-660 nm in Fig. 10 is assigned to the $^5F_5 \rightarrow {}^5I_8$ transition. However, decay curves for the $^5F_5$ level measured at 647.4 and 660.2 nm show significant differences. In fact both are characterized by a non-exponential decay with a 1/e decay time of about 65 μs, but the curve for the 660.2 nm also shows a rise with a time constant of about 7 μs. The same rise time was also observed for emission lines at 375.2, 377.6, 541.8 and 551.6 nm. The presence of this rise could be due either to energy transfer between different Ho^{3+} centres (e.g., ions in different sites, pairs) or to a slow process populating the centres emitting at 660.2 nm upon UV excitation. The decay time constant of the $^5F_5$ level is in both cases close to 65 μs; this value can be compared to a radiative lifetime of 317 μs [9]. The comparison shows that concentration quenching processes are effective, as expected for the high Ho^{3+} concentration.

The weaker emission lines appeared in Fig. 10 around 490 nm are assigned to the $^3F_3 \rightarrow {}^5I_8$ transition. The corresponding decay curve of $^3F_3$ is non-exponential due to cross relaxation with a 1/e decay time of about 4.5 μs. The remaining weak lines at 580.6 and 586.0 nm have the same decay curves with a short decay time of 1.4 μs as the weak 391.0 nm line (Fig. 11 (a)). This is

explained as follows. The former lines are due to the $^5G_4 \rightarrow {}^5I_6$ transition, while the latter line is due to the $^5G_4 \rightarrow {}^5I_8$ transition. The initial excited state is the same ($^5G_4$) for these emission lines.

Figure 12 shows the decay curves at room temperature. All the emission lines show shorter decay times at room temperature than at 17 K, e.g., 1/e decay time of 31 μs for 647.4 and 660.2 nm lines and 3.0 μs for 485.4 and 491.6 nm lines. This is reasonable because non-radiative process enhances at higher temperatures.

4. Conclusions

The near IR luminescence spectroscopy of BaY_2F_8 single crystals heavily doped with the Ho^{3+} ion (10 and 30 mol %) upon excitation in the visible region is characterized by very strong emission bands originating from the first $^5I_7$ level and located around 2070 nm. In these conditions the population of the second emitting state $^5I_6$ appears to be low. However $^5I_7$ emission is not observed upon excitation at wavelengths shorter than 300 nm presumably because at the present doping levels cross relaxation processes bypass the $^5I_7$ level without populating it. A detailed analysis of the excited state dynamics is made particularly complex by the presence of multiple cross relaxation and upconversion pathways made possible by the high Ho^{3+} concentration, and by the possible presence of pairs and clusters of Ho^{3+} ions, and/or of Ho^{3+} ions in minority sites in the crystal structure. The inter-ionic processes are found to shorten the decay times of the levels emitting in the visible region with respect to the corresponding radiative lifetimes. The strong near IR emission from $^5I_7$ indicates that these heavily doped crystals could find be useful as light emitting materials in the 2 μm region.

Acknowledgment

The present work was partly supported by the Grant-in-Aid from Japan Society for the Promotion of Science (JSPS).

References

[1] V. Sudesh, K. Asai, K. Shimamura, T. Fukuda, IEEE J. Quantum Electron. 38 (2002) 1102.
[2] H. Johnson, Lasers in Surgery and Medicine 14 (1994) 213.
[3] M. Schellom, A. Hirth, C. Kieleck, Opt. Lett. 28 (2003) 1933.
[4] S. Polosan, M. Bettinelli, T. Tsuboi, Phys. Stat. Sol. (c) 4 (2007) 1352.

[5] R.L. Remski, L.T. James, K.H. Gooen, B. Di Bartolo, A. Linz, IEEE J. Quantum Electron. QE-15（1969）214.
[6] E.P. Chicklis, C.S. Naiman, R.C. Folweiler, D.R. Gabbe, H.P. Jenssen, A. Linz, Appl. Phys. Lett. 19（1971）119.
[7] E.V. Boiko, V.F. Danilichev, N.N. Smirnov, V.V. Lazo, Proceedings, Conference on Lasers and Electro-Optics Europe（1994）216.
[8] M. Doshida, M. Obara, Jpn. J. Appl. Phys. 34（1995）6079.
[9] A.M. Tkachuk, S.I. Klokishner, A.V. Poletimova, L.M. Mogileva, M.V. Petrov, Opt. Spektrosk. 60（1986）1201.
[10] R. Stutz, H. C. Miller, K. M. Dinndorf, A. Cassanho, H. P. Jenssen, Proceedings of SPIE-The International Society for Optical Engineering, 5332（Solid State Lasers XIII: Technology and Devices）（2004）111.
[11] F. Cornacchia, A. Toncelli, M. Tonelli, Progr. Quantum Electron. 33（2009）61.
[12] A. Gektin, N. Shiran, V. Nesterkina, Y. Boyarintseva, V. Baumer, G. Stryganyuk, K. Shimamura, E. Villora, J. Lumin. 129（2009）1538.
[13] L. H. Guilbert, J. Y. Gesland, A. Bulou, R. Retoux, Mater. Res. Bull. 28（1993）923.
[14] A. A. Kaminskii, Phys. Stat. Solid.（a）148（1995）9.
[15] R. D. Shannon. Acta Cryst. A32（1976）751.
[16] Value calculated from bond length-bond strength equations, see http://abulafia.mt.ic.ac.uk/shannon/.
[17] G. H. Dieke, Spectra and Energy Levels of Rare Earth Ions in Crystals, edited by H.M. Crosswhite and H. Crosswhite, Wiley Interscience Publishers,（New York, 1968）.
[18] W. T. Carnall, H. Crosswhite and H. M. Crosswhite, Energy Level Structure and Transtion Probabilities of the Trivalent Lanthanides in LaF_3, Report Argonne National Laboratory, Chemistry Division, Argonne（Illinois）, 1977.
[19] R. T. Wegh, A. Meijerink, R.-J. Lamminmäki, J. Hölsä, J. Lumin. 87-89（2000）1002.
[20] P. S. Peijzel, R. T. Wegh, A. Meijerink, J. Hölsä, R.-J. Lamminmäki, Optics Comm. 204（2002）195.
[21] E. Osiac, I. Sokólska, S. Kück, J. Alloys Comp. 323-324（2001）283.
[22] M. B. Seelbinder, J.C. Wright, Phys. Rev. B 20（1979）4308.
[23] E. Osiac, I. Sokólska, S. Kück, Phys. Rev. B 65（2002）235119.
[24] M. Malinowski, M. Kaczkan, S. Stopiński, R. Piramidowicz, A. Majchrowski, J. Lumin. 129（2009）1505.
[25] M. Kowalska, G. Klocek, R. Piramidowicz, M. Malinowski, J. Alloys Comp. 380（2004）156.
[26] M. Kaczkan, M. Malinowski, J. Alloys Comp. 380（2004）201.

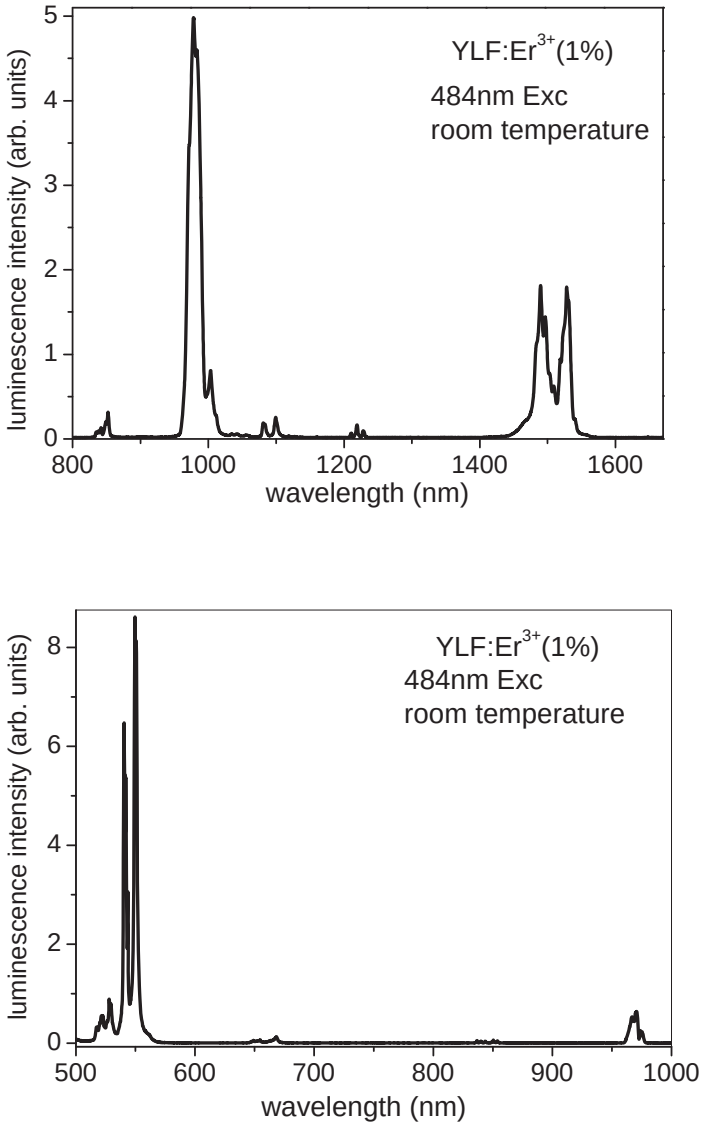

Fig. 1 Near infrared luminescence spectrum of 1% Er^{3+} -doped $LiYF_4$ (YLF) crystal at room temperature upon excitation at 484 nm.

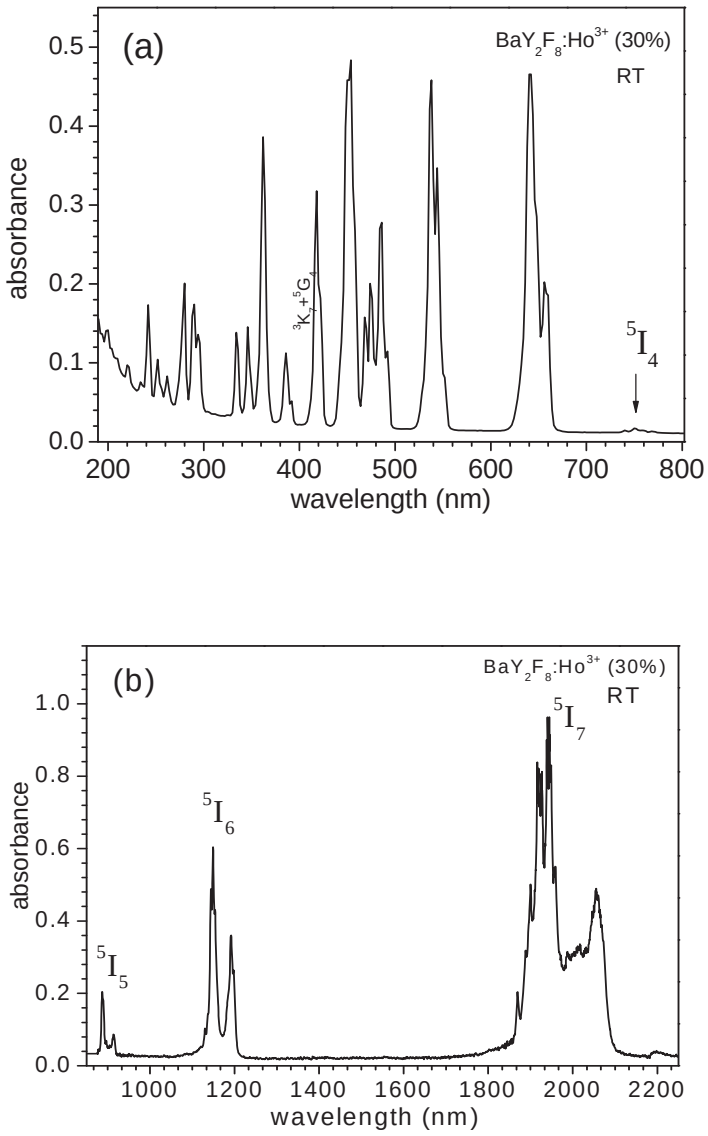

Fig. 2 Ultraviolet-visible (a) and near infrared (b) absorption spectra of Ho^{3+} ions in 30% Ho^{3+} -doped BaY_2F_8 crystal at room temperature. The thickness of crystal is 2 mm.

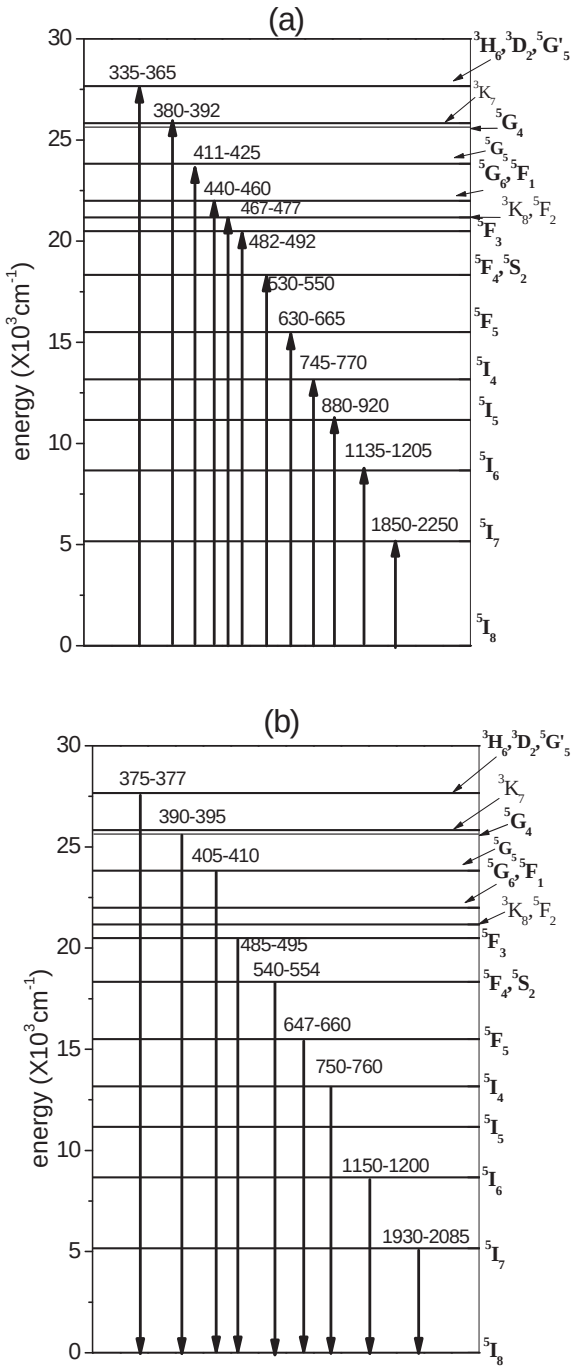

Fig. 3 Energy level assignment and observed absorption (a) and emission (b) bands due to the Ho^{3+} ion in BaY_2F_8. Number such as 1930-2085 in (b) means emission band appeared between 1930 and 2085 nm.

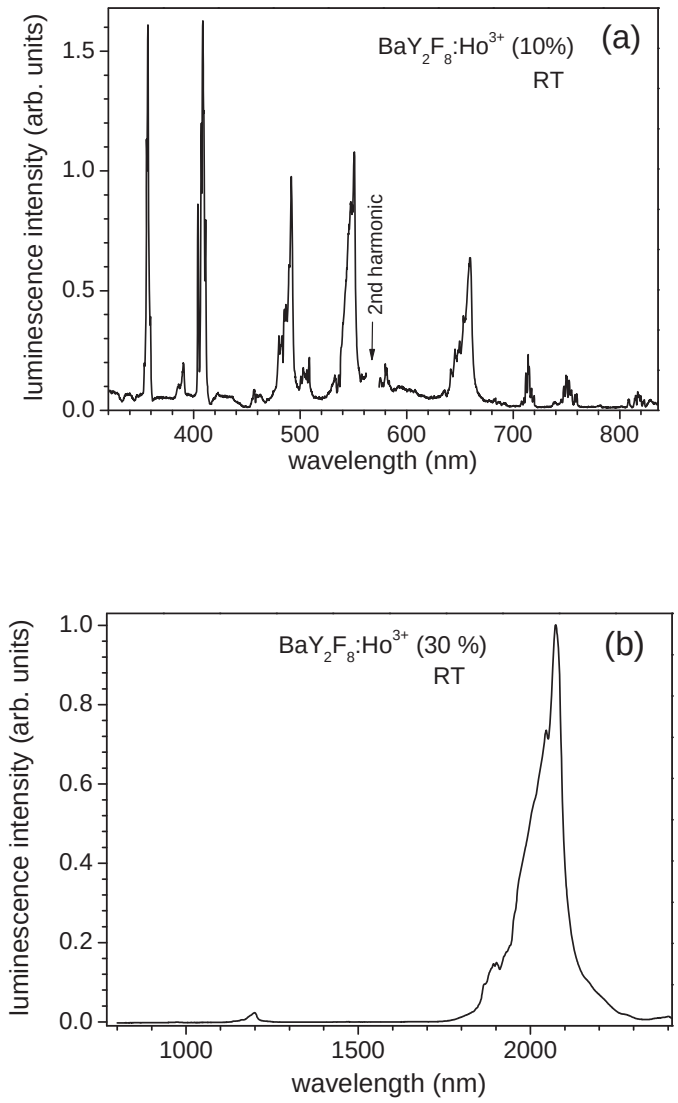

Fig. 4 Luminescence spectra of 10% Ho^{3+} -doped BaY_2F_8 crystal at room temperature. (a) Spectral range 300-850 nm obtained upon excitation at 285 nm. The spectral range of 555-575 nm is deleted because of an intense band due to the second harmonic of the 285 nm excitation light. (b) Spectral range of 800-2400 nm obtained upon excitation at 360 nm.

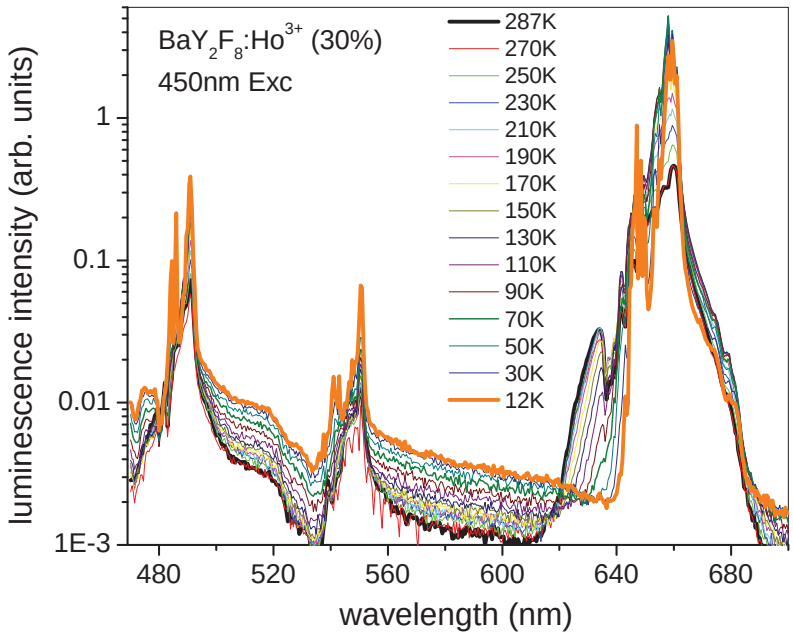

Fig. 5 Luminescence spectra, in a visible spectral range, of 30% Ho^{3+} -doped BaY_2F_8 crystal excited at 450 nm at various temperatures.

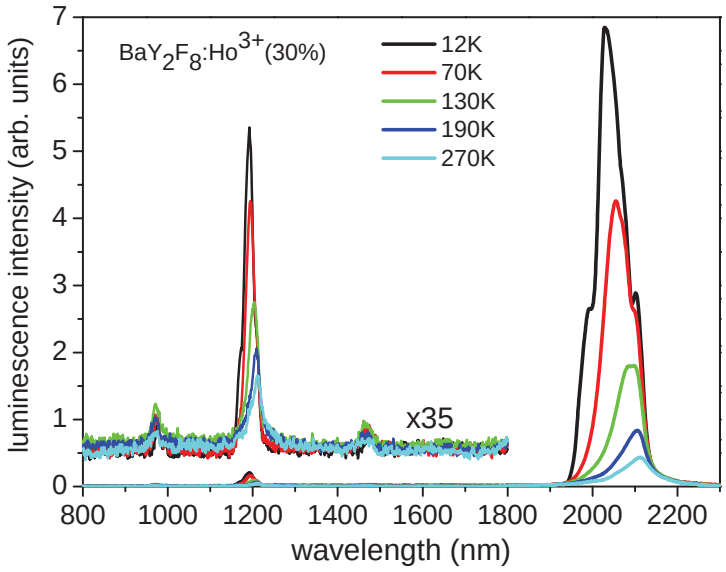

Fig. 6 Near infrared emission spectra of 30% Ho^{3+} -doped BaY_2F_8 crystal excited at 360 nm at various temperatures. Inset is the extended spectra（by 35 times）at 800-1800 nm.

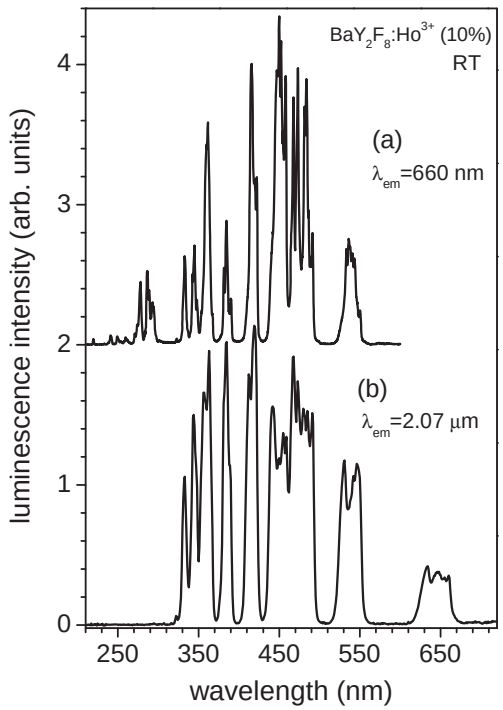

Fig. 7 Excitation spectra for 660 nm emission (a) and for 2070 nm emission (b) of the 10% Ho^{3+} -doped BaY_2F_8 crystal at room temperature.

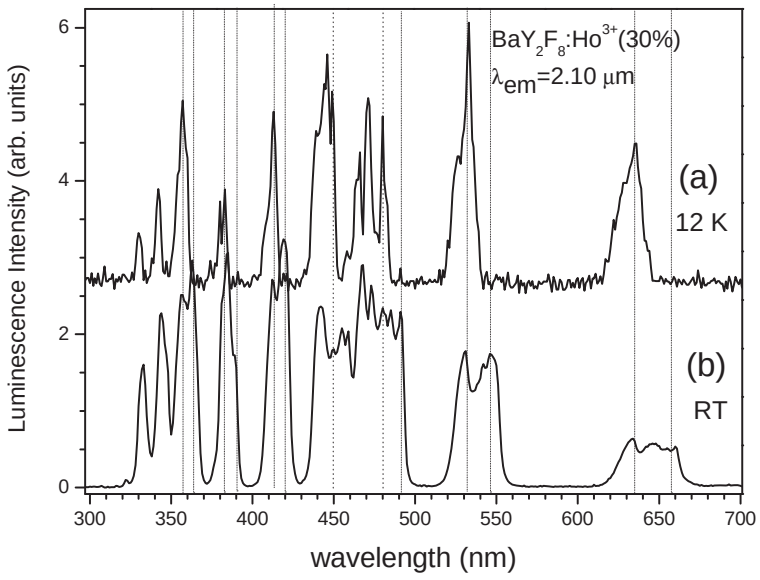

Fig. 8 Excitation spectra for the 2070 nm emission of 30% Ho^{3+} -doped BaY_2F_8 crystal at 12 K (a) and room temperature (b).

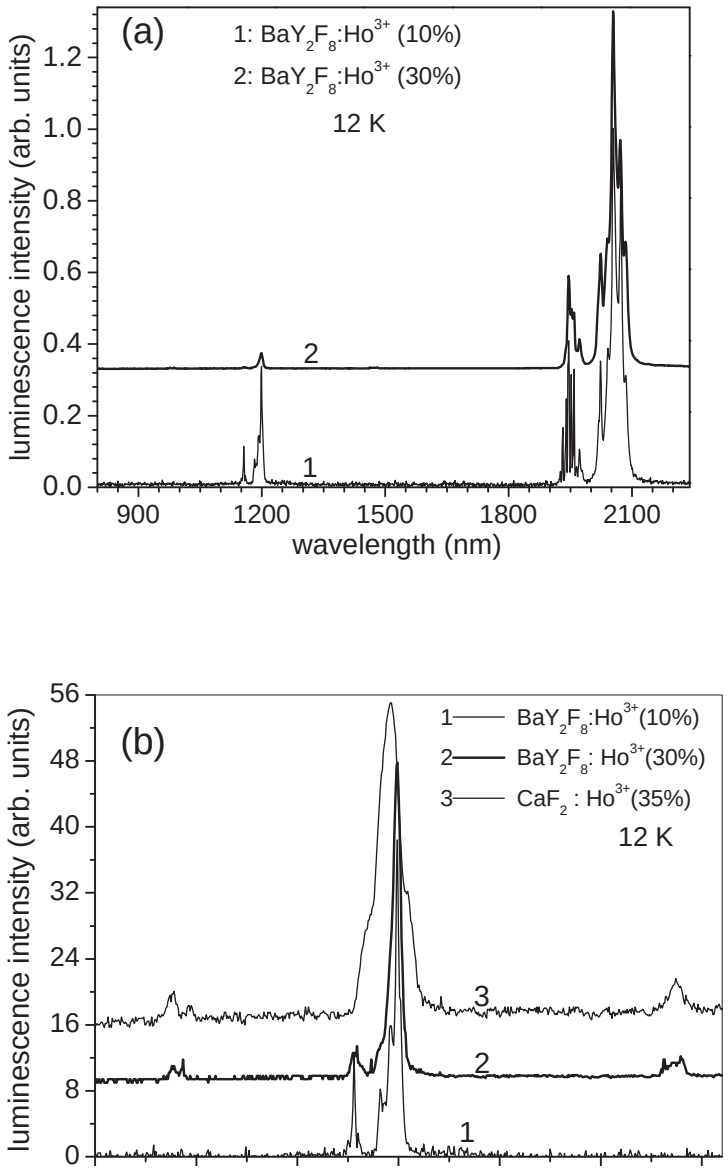

Fig. 9 (a) Near-infrared luminescence spectra of 10% and 30% Ho^{3+} -doped BaY_2F_8 crystals which were excited at 447 nm at 12 K. (b) Near-infrared PL spectra of 10% and 30% Ho^{3+} -doped BaY_2F_8 and 35% Ho^{3+} -doped CaF_2 crystals which were excited at 447 nm at 12 K. The (a) and (b) figures are normalized at the 2054 and 1190 nm PL peaks, respectively. The spectra are shifted upwards for comparison.

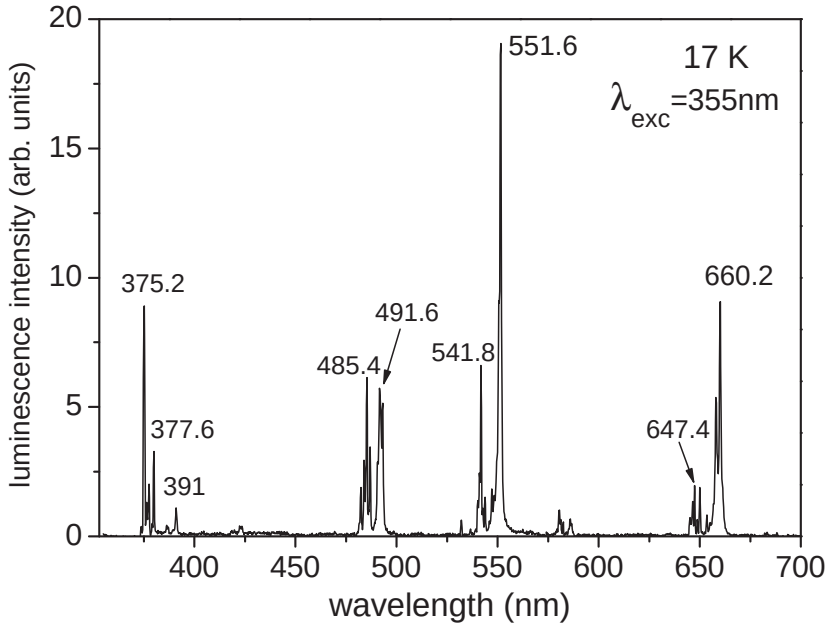

Fig. 10 Highly-resolved PL spectrum of 10 % Ho^{3+} -doped BaY_2F_8 crystal at 17 K.

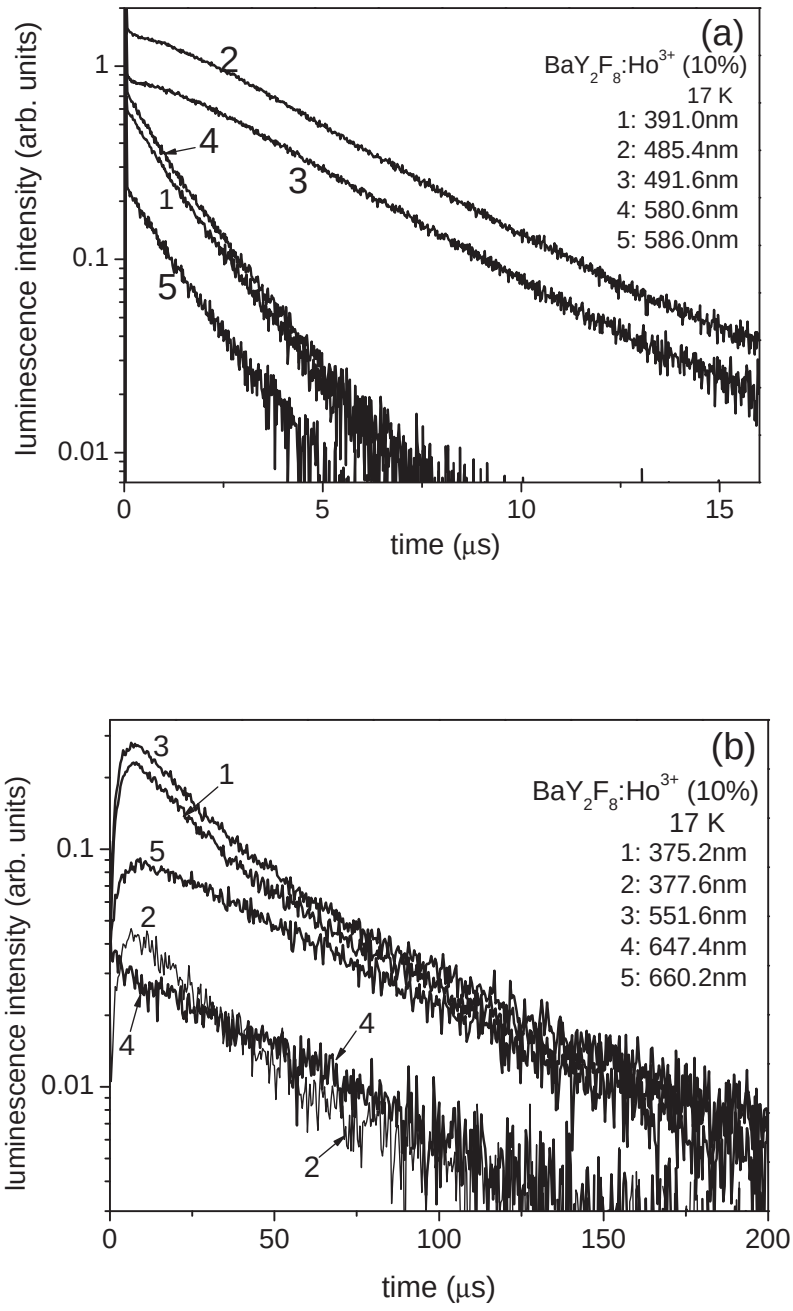

Fig. 11 Decay curves of various emission lines shown in Fig.10, measured with a 355 nm laser pulsed excitation at 17 K with time scales of（a）0-18 μs and（b）0-300 μs.

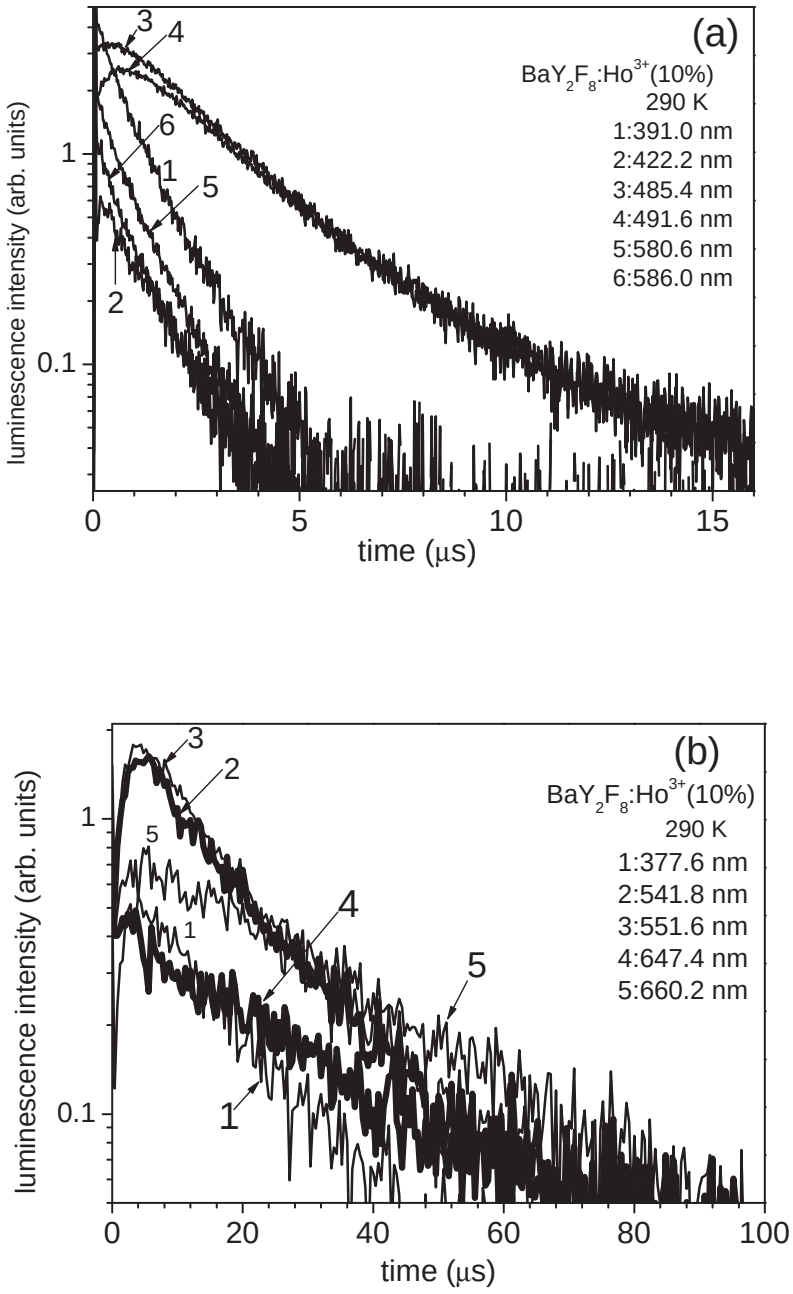

Fig. 12 Decay curves of various emission lines, measured with a 355 nm laser pulsed excitation at 290 K with time scales of (a) 0-18 μs and (b) 0-300 μs.